UCLA
COMPUTATIONAL AND APPLIED MATHEMATICS

Advanced in Boundary Layer Control: Robust Reduced-Order Transition Controller

L. Cortelezzi
J.L. Speyer

December 1997

CAM Report 97-57

Department of Mathematics
University of California, Los Angeles
Los Angeles, CA. 90095-1555

Advance in Boundary Layer Control: Robust Reduced-Order Transition Controller

by L. CORTELEZZI,[1,2] * J.L. SPEYER[2]

[1] Department of Mathematics
University of California, Los Angeles, California 90095-1555
[2] Department of Mechanical and Aerospace Engineering
University of California, Los Angeles, California 90095-1597

December 22, 1997

PACS NUMBERS: 47.62.+q, 47.27.Cn, 47.27.Rc, 47.27.Vf., 07.05.Dz

Abstract

A framework to derive optimal and robust reduced-order controllers of transitional boundary layers using linear-quadratic-Gaussian (LQG) design, or, in modern terms, $\mathcal{H}_2$ design, is presented. As a test case, two-dimensional Poiseuille flow is considered. A controller based on a reduced model, 8% of the order of the full size system, is designed. Initial conditions creating transient growth of wall-shear stresses are constructed. The controller is tested on a 32 wave numbers simulation. Wall-shear stresses reduction, up to 90%, is obtained. The transferability of the controller to Navier-Stokes simulations and engineering applications is discussed.

*Corresponding author: Telephone (310) 206-2732, Facsimile (310) 206-6673, E-mail: crtlz@math.ucla.edu

The reduction of drag produced by skin friction, or, in other words, the reduction of wall-shear stresses (WSS) generated by near-wall turbulence have received wide attention. "The skin friction constitutes about 50%, 90%, and 100% of the total drag on commercial aircraft, underwater vehicles, and pipelines, respectively."[1] Two are the near-wall flows of interest: boundary layers that transition from laminar to turbulent regime and boundary layers that are inherently turbulent. Correspondly, efforts of reducing skin friction fall in two broad categories: transition inhibition and turbulence suppression. References 1-3 are recent reviews summarizing achievements and open questions in boundary layer control.

Boundary layer control has been attempted with some success. It is becoming widely accepted that even better results could be obtained by using controllers able to analyze distributed measurements and coordinate distributed actuators. Interestingly enough, however, very little has been done to exploit the tools developed in the control community.[4-6] In particular, linear-quadratic-Gaussian (LQG) design, or, in modern terms, $\mathcal{H}_2$ design, combined with model reduction techniques for multi-inputs-multi-outputs (MIMO) systems has never been explored.

This letter shows that MIMO LQG ($\mathcal{H}_2$) design can be successfully applied to derive an optimal and robust reduced-order controller able to suppress up to 90% WSS in a two-dimensional Poiseuille flow. This letter also addresses the transferability of the controller to numerical simulations and engineering applications. Finally, this letter provides guidelines for the application of LQG ($\mathcal{H}_2$) and model reduction to other flows described by partial-differential equations.

We consider two-dimensional incompressible Poiseuille flow in a periodic channel of length Lh and height $2h$. The undisturbed velocity field has a parabolic profile $U(y) = U_c(y^2 - h^2)$, where U_c is the velocity at the centerline. Since we are interested in controlling the transition of the boundary layer from laminar to turbulent regime, we consider small perturbation of flow quantities. Let ψ be the perturbation stream-function. The linearized Navier-Stokes equations are written in terms of the stream-function to identically satisfy continuity,

$$(\frac{\partial}{\partial t} + U\frac{\partial}{\partial x}) \triangle \psi - \frac{d^2U}{dy^2}\frac{\partial \psi}{\partial x} = \frac{1}{Re} \triangle \triangle \psi. \tag{1}$$

The problem is made dimensionless by using h as characteristic length and h/U_c as characteristic time. The Reynolds number is $Re = U_c h/\nu$.

To suppress perturbations evolving within the bottom boundary layer we apply blowing and suction at the bottom wall (see Figure 1). For simplicity we assume that the actuators are uniformly distributed. The top boundary layer is left free to evolve. The corresponding boundary conditions are

$$\left.\frac{\partial \psi}{\partial x}\right|_{y=-1} = -v_w(x,t), \qquad \left.\frac{\partial \psi}{\partial y}\right|_{y=\pm 1} = \psi(x,1,t) = 0, \tag{2}$$

where the control function v_w prescribes the amount of blowing and suction at the bottom wall. We impose that the mass of fluid injected equals the mass of fluid removed.

To detect and measure the deviations of the boundary layer from the laminar regime, we measure the gradient of the streamwise velocity component, or WSS, at given points $x = x_i$ along the bottom wall (see Figure 1)

$$z(x_i,t) = \left.\frac{\partial^2 \psi}{\partial y^2}\right|_{y=-1}. \tag{3}$$

We define an optimal performance index, or cost function, to design a controller for the LQG ($\mathcal{H}_2$) problem. Since we are interested in suppressing WSS, a natural choice is the following

$$J = \lim_{t_f \to \infty} \int_t^{t_f} \int_0^L \left[\left(\left.\frac{\partial^2 \psi}{\partial y^2}\right|_{y=-1} \right)^2 + W v_w^2 \right] dx\,dt. \tag{4}$$

The term $(\partial^2\psi/\partial y^2)^2$ represents the cost of the WSS being different from zero while the term v_w^2 represents the cost of implementing the control itself. The design parameter W balances the amount of control effort against the reduction of WSS. There are two reasons to minimize the cost of the controller: In any engineering application the energy available to drive the controller is limited; and a large control action may drive the system away from the region where the linear model is valid.

To reduce (1)-(3) to a set of first-order ordinary differential equations, we make a few transformations loosely based on the approach presented in Ref. 4 and 5. A modified stream function ϕ is introduced to embed the actuator into the evolution equation and to make the boundary conditions homogeneous. Flow quantities are expanded as follows: $\phi = \sum_{n=1}^{N} \sum_{m=0}^{M} [a_{nm}(t)\cos(n\alpha_0 x) + b_{nm}(t)\sin(n\alpha_0 x)]C_m(y)$, $v_w = \sum_{n=1}^{N} n\alpha_0 [p_n(t)\sin(n\alpha_0 x) - q_n(t)\cos(n\alpha_0 x)]$, $z = \sum_{n=1}^{N} [c_n(t)\cos(n\alpha_0 x) +$

$d_n(t)\sin(n\alpha_0 x)]$, where C_m are basis functions constructed using Chebyshev polynomials.[4,5] Finally, we use Galerkin's projection and a linear transformation to make (1)-(3) into the following state-space form

$$\frac{d\boldsymbol{x}}{dt} = \boldsymbol{A}\,\boldsymbol{x} + \boldsymbol{B}\,\boldsymbol{u}\,, \qquad \boldsymbol{z} = \boldsymbol{C}\,\boldsymbol{x} + \boldsymbol{D}\,\boldsymbol{u}\,, \tag{5}$$

with initial condition $\boldsymbol{x}\,(0) = \boldsymbol{x_0}$; where $\boldsymbol{x}$ is the internal state vector, $\boldsymbol{u}$ is the control vector and $\boldsymbol{z}$ is the measurement vector. The cost function (4) becomes

$$J = \lim_{t_f \to \infty} \int_t^{t_f} [\boldsymbol{x}^{\,T}\boldsymbol{C}^{\,T}\boldsymbol{C}\,\boldsymbol{x} + 2\boldsymbol{x}^{\,T}\boldsymbol{C}^{\,T}\boldsymbol{D}\,\boldsymbol{u} + \boldsymbol{u}^{\,T}(\boldsymbol{D}^{\,T}\boldsymbol{D} + \boldsymbol{W})\boldsymbol{u}\,]dt, \tag{6}$$

where the superscript $^{\,T}$ denotes transpose. The matrix $\boldsymbol{W}$ is an appropriate weight for the cost of the controller.

The advantage of the present formulation is that the problem decouples with respect to the wave number. All matrices in (5) and (6) are block diagonal. The block diagonal structure of the matrix $\boldsymbol{A}$ was first recognized in Ref. 4. The above state-space system is consequently equivalent to N state-space sub-systems, one for each wave number. For a given wave number r the state-space equations are

$$\frac{d\boldsymbol{x_r}}{dt} = \boldsymbol{A_r}\,\boldsymbol{x_r} + \boldsymbol{B_r}\,\boldsymbol{u_r}\,, \qquad \boldsymbol{z_r} = \boldsymbol{C_r}\,\boldsymbol{x_r} + \boldsymbol{D_r}\,\boldsymbol{u_r}\,, \tag{7}$$

with initial condition $\boldsymbol{x_r}\,(0) = \boldsymbol{x_{r0}}$. Vectors $\boldsymbol{x_r}\,, \boldsymbol{u_r}\,, \boldsymbol{z_r}$ have the following structure: $\boldsymbol{x_r} = [a_{r0}, \cdots a_{rM}, b_{r0}, \cdots b_{rM}]^T, \boldsymbol{u_r} = [p_r, q_r]^T, \boldsymbol{z_r} = [c_r, d_r]^T$. The cost function also decouples with respect to the wave number and we obtain N optimal performance indexes. For a given wave number r the cost function is defined as follows

$$J_r = \lim_{t_f \to \infty} \int_t^{t_f} [\boldsymbol{x_r}^{\,T}\boldsymbol{C_r}^{\,T}\boldsymbol{C_r}\,\boldsymbol{x_r} + 2\boldsymbol{x_r}^{\,T}\boldsymbol{C_r}^{\,T}\boldsymbol{D_r}\,\boldsymbol{u_r} + \boldsymbol{u_r}^{\,T}(\boldsymbol{D_r}^{\,T}\boldsymbol{D_r} + \boldsymbol{W_r})\boldsymbol{u_r}\,]dt. \tag{8}$$

Consequently, the design of an optimal and robust controller for the system (5) with (6) has been reduced to the independent design of N optimal and robust controllers, one for each wave number, for the sub-systems (7) with (8).

The challenge of the present study is to reduce of the size of the controller. The controller of the full system would have $2N(M+1)$ states, where N=32 and M=64 in the simpler cases considered in

literature. A controller with thousands of states is of no interest in engineering applications because of the amount of hardware and computer power necessary to compute a real-time control law. We derive a lower order controller in two steps: First we construct a lower order model of (7), and subsequently, we design an optimal and robust controller for the reduced-order model. To obtain a lower order model, we transform (7) into Jordan Canonical form and subsequently retain only the states that are equally well controllable and observable. In practice, the matrices $\hat{\boldsymbol{A}}_r$, $\hat{\boldsymbol{B}}_r$, $\hat{\boldsymbol{C}}_r$, $\boldsymbol{D}_r$ that describe the dynamics of the reduced-order model are obtained from the matrices in Jordan Canonical form by removing rows and columns corresponding to the unnecessary states. Hat denotes the quantities associated with the reduced-order model.

Control theory provides a framework for designing optimal and robust controllers.[7,8] The design of an optimal and robust controller for the LQG ($\mathcal{H}_2$) problem is divided in two parts: the linear quadratic regulator (LQR) and the minimum variation estimator (Kalman-Bucy filter). LQR provides an optimal control law in terms of the internal state vector. In general, however, the internal state vector is not directly measurable. The Kalman-Bucy filter provides an optimal estimate of the internal state vector in terms of the measurements vector $\boldsymbol{z}_r$. The result of the LQG ($\mathcal{H}_2$) design of an optimal and robust controller based on the reduced-order model of (7) is summarized by the following equations:

$$\boldsymbol{u}_r = -\hat{\boldsymbol{K}}_r \, \tilde{\boldsymbol{x}}_r \, , \tag{9}$$

$$\frac{d\tilde{\boldsymbol{x}}_r}{dt} = \hat{\boldsymbol{A}}_r \, \tilde{\boldsymbol{x}}_r + \hat{\boldsymbol{B}}_r \, \boldsymbol{u}_r + \hat{\boldsymbol{L}}_r \, [\boldsymbol{z}_r - \hat{\boldsymbol{C}}_r \, \tilde{\boldsymbol{x}}_r - \boldsymbol{D}_r \, \boldsymbol{u}_r \,], \tag{10}$$

with initial conditions $\tilde{\boldsymbol{x}}_r \, (0) = \boldsymbol{0}$. The gains matrix $\hat{\boldsymbol{K}}_r$ is obtained by minimizing the following optimal performance index:

$$\hat{J}_r = \lim_{t_f \to \infty} \int_t^{t_f} [\hat{\boldsymbol{x}}_r{}^T \hat{\boldsymbol{C}}_r{}^T \hat{\boldsymbol{C}}_r \, \hat{\boldsymbol{x}}_r + 2\hat{\boldsymbol{x}}_r{}^T \hat{\boldsymbol{C}}_r{}^T \boldsymbol{D}_r \, \boldsymbol{u}_r + \boldsymbol{u}_r{}^T (\boldsymbol{D}_r{}^T \boldsymbol{D}_r + \boldsymbol{W}_r) \boldsymbol{u}_r \,] dt. \tag{11}$$

Equation (9) is the control law. Equation (10) is the the minimum variation estimator. The matrix $\hat{\boldsymbol{L}}_r$ is obtained by minimizing the variance of the estimated state vector $\tilde{\boldsymbol{x}}_r$ with respect to the internal state vector $\hat{\boldsymbol{x}}_r$ assuming that the reduced-model of (7) is affected by additive Gaussian white noise. In this study the power spectral densities of the additive noise are used as design parameters to

produce robust controllers. The initial condition $\tilde{\boldsymbol{x}}_r\ (0) = \mathbf{0}$ implies that the estimator starts with no information about $\hat{\boldsymbol{x}}_r$.

Figure 1 summarizes in a block diagram the control strategy described above. Note that the numerical integration of the estimator (10), the computation of the control law (9), and fast direct and inverse Fourier transforms can be programmed in a computer routine. Subsequently, this routine can be embedded in any Navier-Stokes solver for the control of more realistic transitional boundary layers. Figure 1 also provides the basic architecture for the implementation of the present controller in practical engineering applications. The WSS can be measured by micro-electro-mechanical-systems (MEMS) hot film sensors.[9] Analog to digital converters (A/D) and digital signal processors (DSP) convert the measured WSS into $\boldsymbol{z}_r$. Each pair of estimator (10) and control (9) blocks is replaced by a microprocessor, and a parallel computation produces $\boldsymbol{u}_r$. A DSP and a digital to analog converter (D/A) produce the actuating signal. Finally, MEMS technology will provide the necessary hardware. Note that a variety of actuators can mimic small amplitude blowing and suction at the wall: porous walls, micro pumps, deformable walls and thermal actuators.[9]

We use a combination of unsteady modes and transient growth to create a worse scenario test case. We choose the Reynolds number and channel length in order to have at least a few unstable modes. The non-orthogonality of the eigenfunctions associated with (1) permits constructing initial conditions leading to transient growth, see Ref. 3 for references. We obtain initial conditions specifically able to generate transient growth of the WSS, instead of internal energy, by modifying a technique proposed in Ref. 10. Although transient growth will be eventually subdued by the viscous effects, it permits testing the capability of the controller in suppressing disturbances that can trigger nonlinear effect and transition to turbulence. Note that this initial condition stimulates modes that are not included in the reduced-order model, and consequently, cannot be directly controlled.

We design a controller for two-dimensional Poiseuille flow in a periodic channel of length $L = 20/\pi$ at $Re = 10000$. The wave numbers corresponding to $N = 8, 9$, and 10 are unstable. We used a grid resolution of $N = 32$ and $M = 124$, consequently, the order of the full system is 8000. Using the

model reduction technique previously described, we create a reduced model of order 640. We derive 32 controllers, one for each wave number. Controllers operate in parallel. Figure 2(a) shows the temporal evolution of WSS along the bottom wall of the channel for the uncontrolled case. The WSS present a rich structure because of the transient growth of 32 stable and unstable wave numbers. Figures 2(b)-(c) show the temporal evolution of the controlled WSS and of the blowing and suction along the bottom wall of the channel. Although the estimator starts with no information about the internal state of the system, the controller reduces the initial WSS in the first few time steps. Subsequently, the amplitude of blowing and suction rises to suppress the effects of transient growth. Eventually, blowing and suction decreases as the transient growth subdues. Controlled WSS show only some low amplitude ripples during the entire simulation. Figure 2(d) shows a comparison of average WSS in the controlled and uncontrolled case. In the uncontrolled case, the average WSS rises sharply due to the transient growth. It fluctuates around its maximum value and, eventually, subsides due to the viscous effects. In the controlled case, the average WSS drops to half of its initial value in the first few time steps after which it decreases with some mild fluctuations. The comparison of the two curves shows up to 90% average WSS reduction. The remaining unsuppressed WSS are due to the modes that cannot be controlled. The performance of the controller can be improved at the price of increasing its order.

In conclusion, we presented a framework to design an optimal and robust reduced-order controller able to suppress up to 90% WSS in a two-dimensional Poiseuille flow. This controller can be programmed in a computer routine whose inputs are the WSS measurements and whose outputs are the blowing and suction at the wall. This routine, suited for parallel computing, can be embedded in any Navier-Stokes solver for the control of more realistic two-dimensional transitional boundary layers. We also presented a plausible hardware architecture for the implementation of the controller in engineering applications. A more complete report with a detailed derivation of the controller and applications to Navier-Stokes simulations is in preparation. Extensions of LQG ($\mathcal{H}_2$) design and applications of $\mathcal{H}_\infty$ design[7,8] to three-dimensional Poiseuille flow and two- and three-dimensional Blasius boundary layers are in progress.

Acknowledgment

The authors thank Dr. J. Kim, Dr. R.T. MCloskey, Dr. J. Burns and Dr. S. Joshi for the enlighting discussions. This work is supported by AFOSR Grant F49620-97-1-0276 and by NASA Grant NCC 2-374 Pr 41.

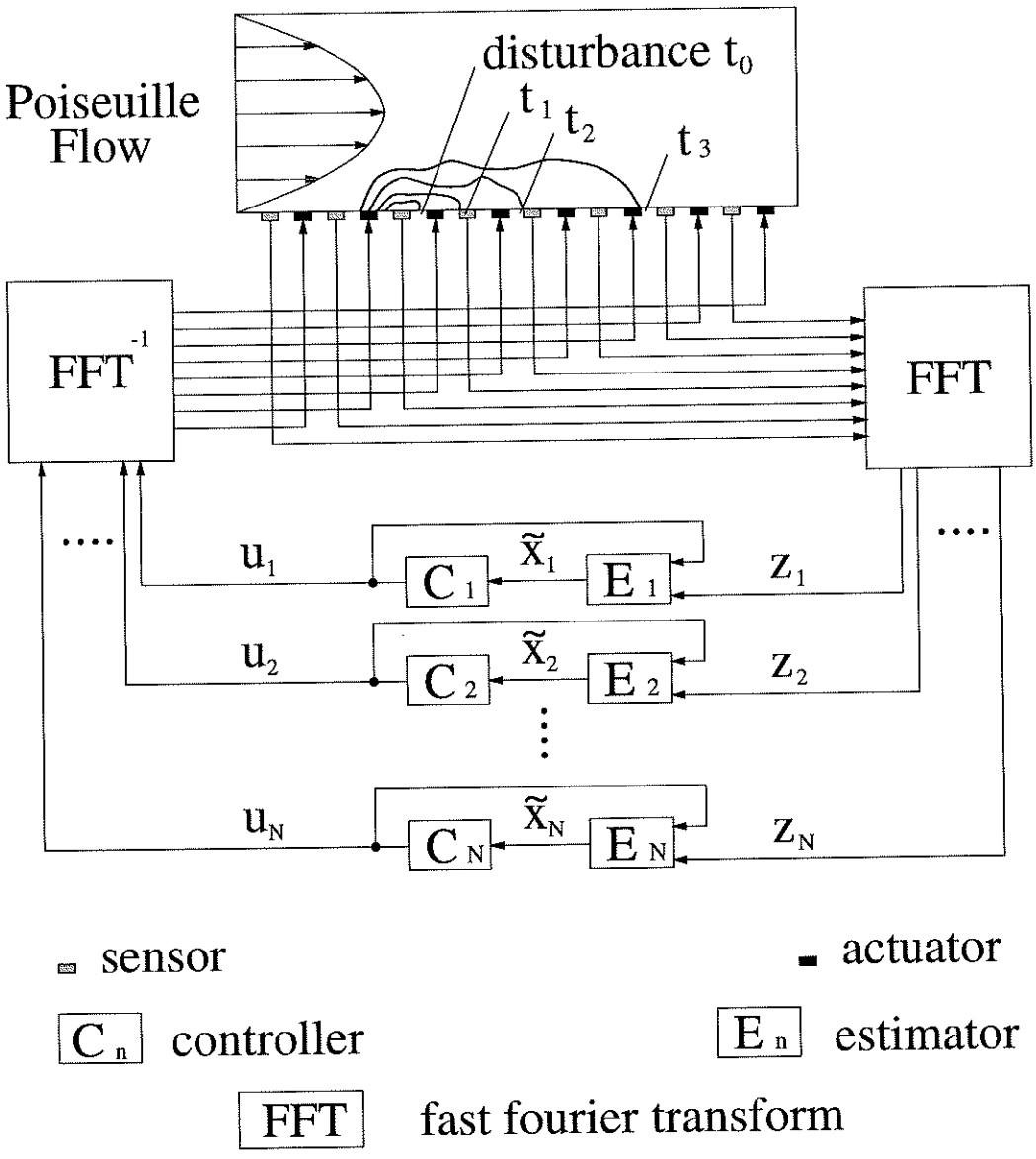

Figure 1: Controller architecture.

(a)

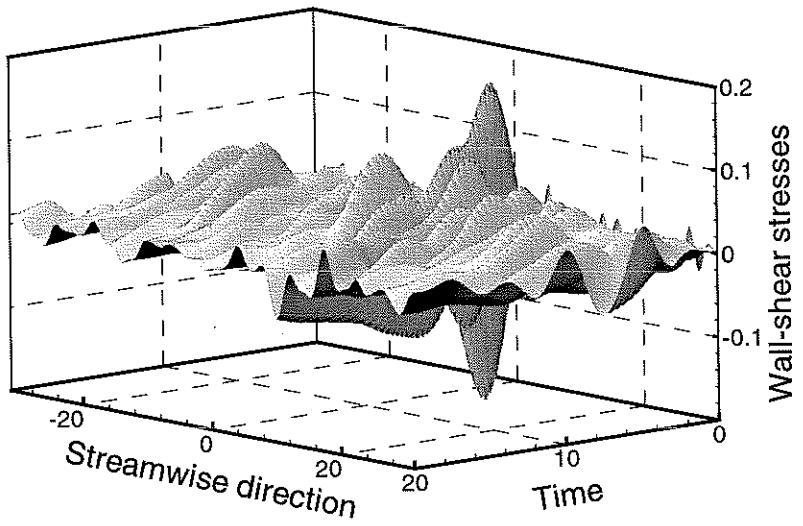

(b)

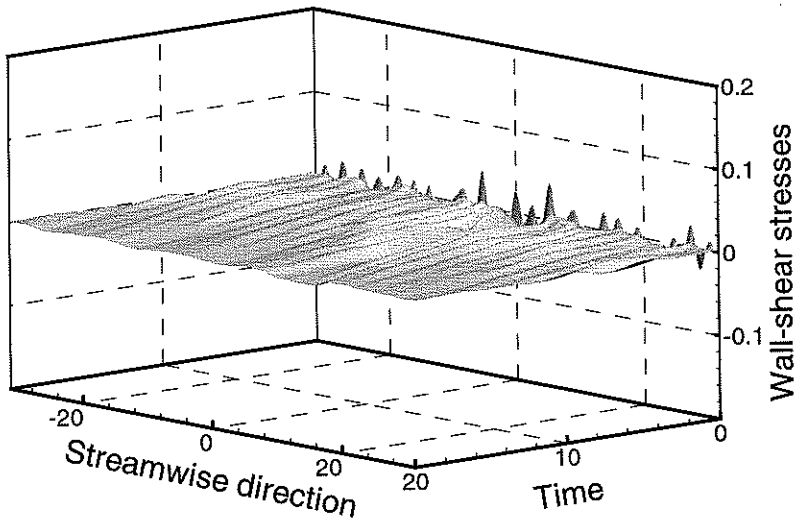

Figure 2: Temporal evolution of wall-shear stresses along the bottom wall of the channel: uncontrolled case (a), controlled case(b).

(c)

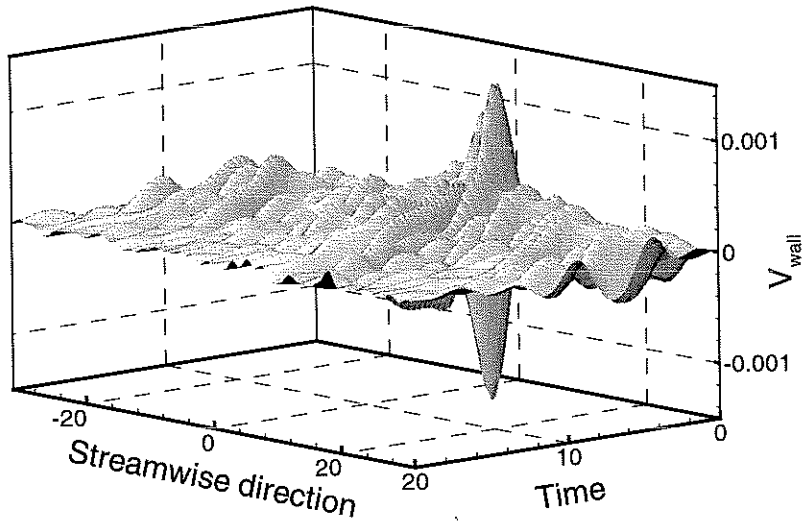

(d)

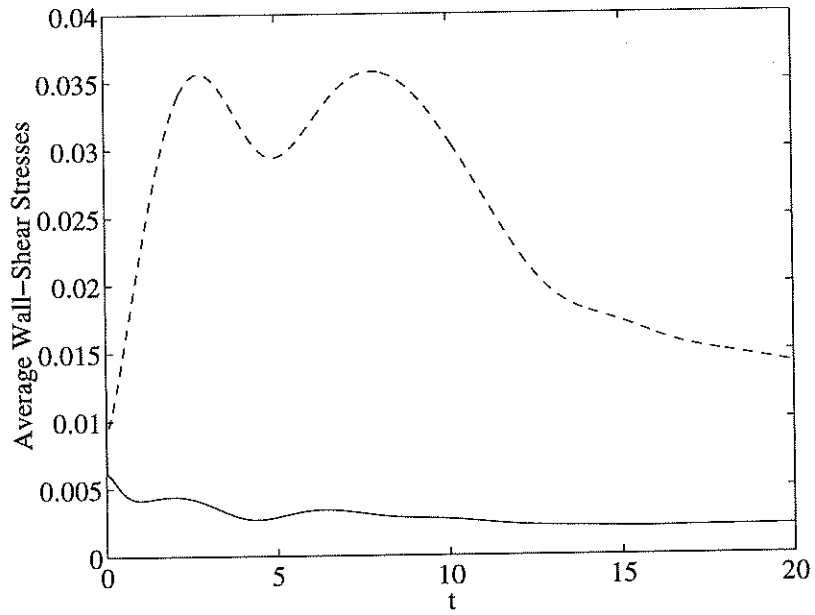

Figure 2: (Continued) Temporal evolution of blowing-suction along the bottom wall of the channel (c). Comparison of average wall-shear stresses in the controlled (solid) and uncontrolled (dashed) case (d).